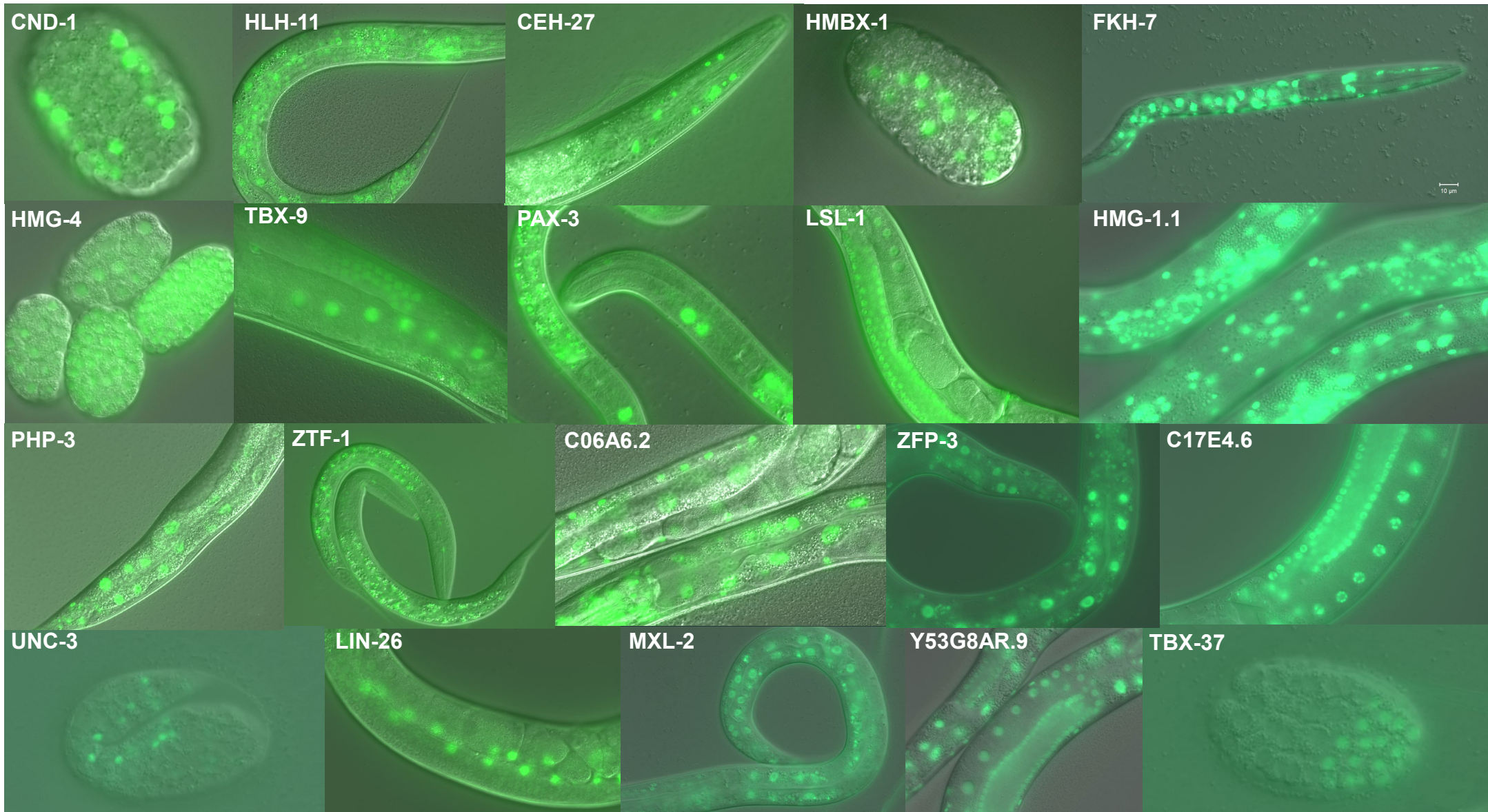


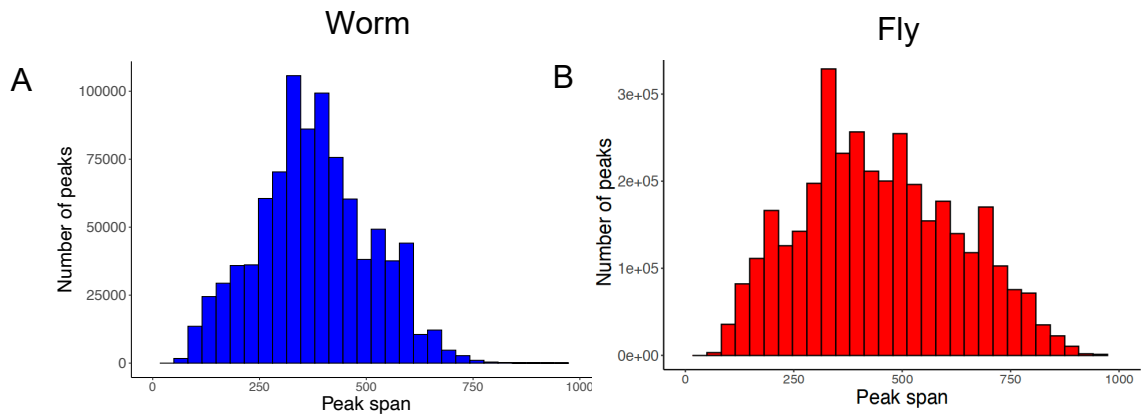
Supplemental Figure 1



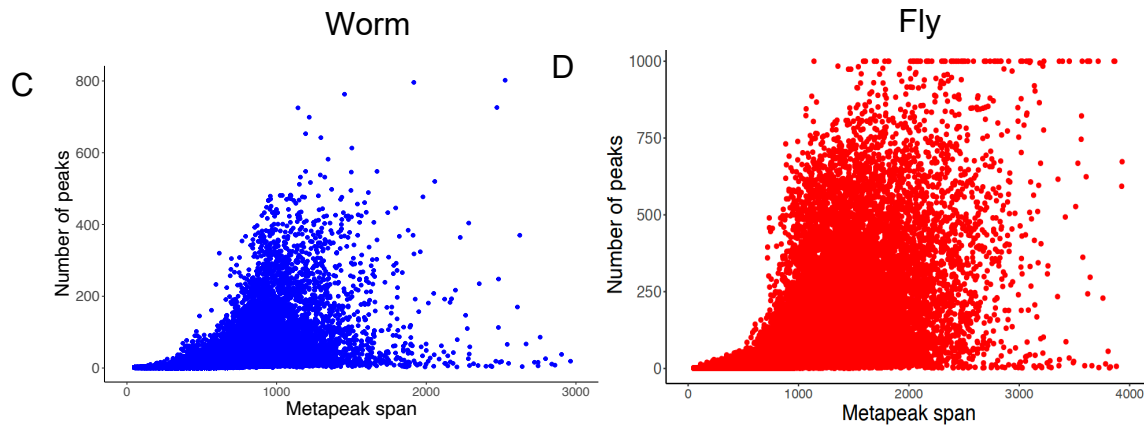
Supplemental Figure 1. Worm TF Expression. Expression patterns of several worm TFs showing the diversity of expression. Shown are merged GFP and DIC images.

Supplemental Figure 2

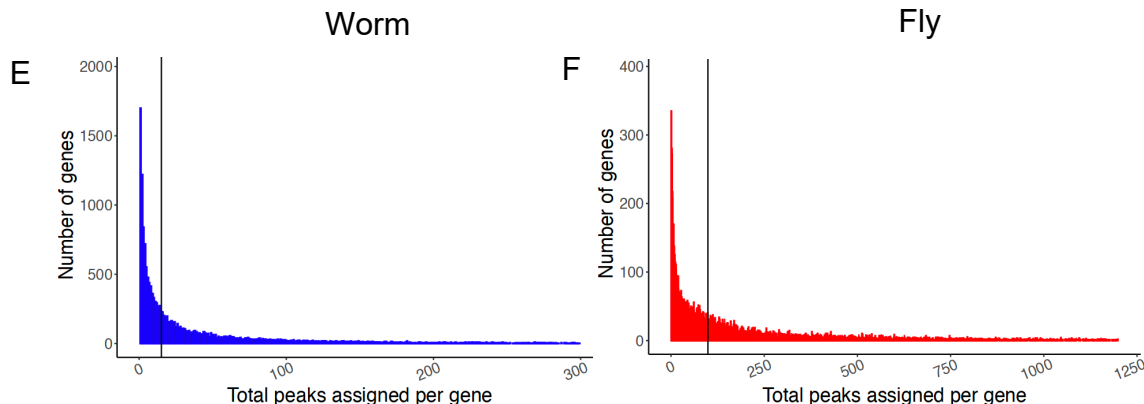
Lengths of peaks



Lengths of metapeaks



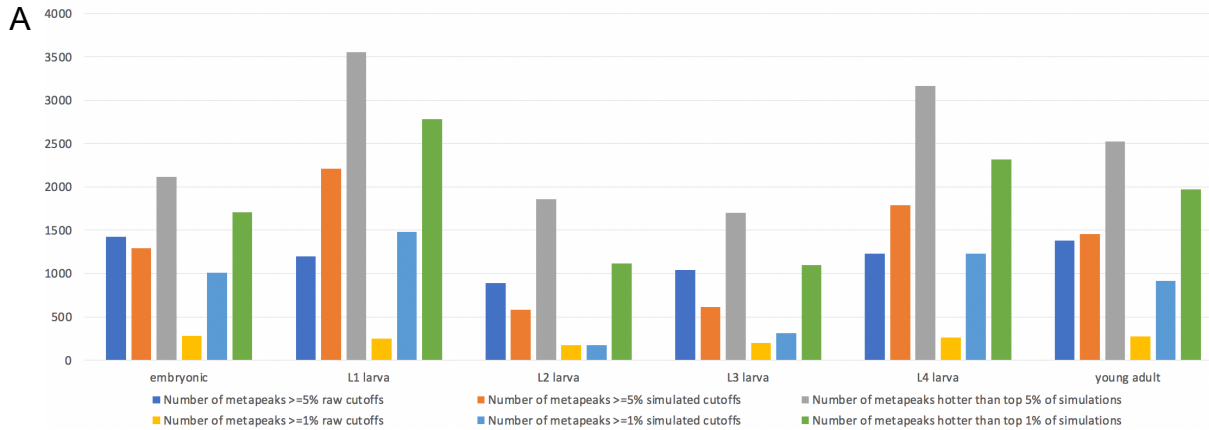
Number of peaks per gene



Supplemental Figure 2. Peak features. **A, B.** The distribution of individual peak lengths in both worm and fly. **C, D.** The span of metapeaks increases only slightly with increased metapeak occupancy in worm (left) and fly (right), with almost all metapeaks less than 2 kb in the worm and less than 3 kb in the fly. **E, F** The number of peaks associated with each gene varies widely, with most genes having relatively few associated peaks, but with many with large numbers of associated peaks. The median number (vertical lines) of peaks per gene in worm was 15 and in fly 99.

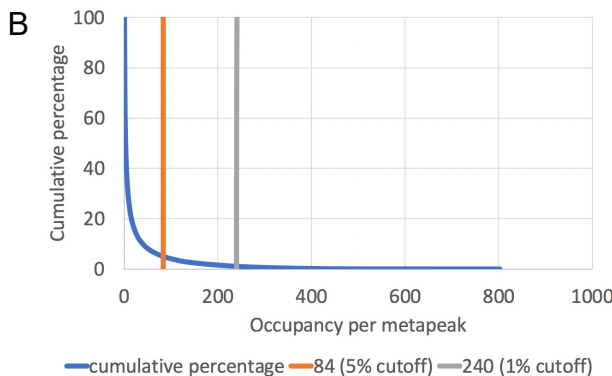
Supplemental Figure 3

Comparison of HOT site thresholds in worm

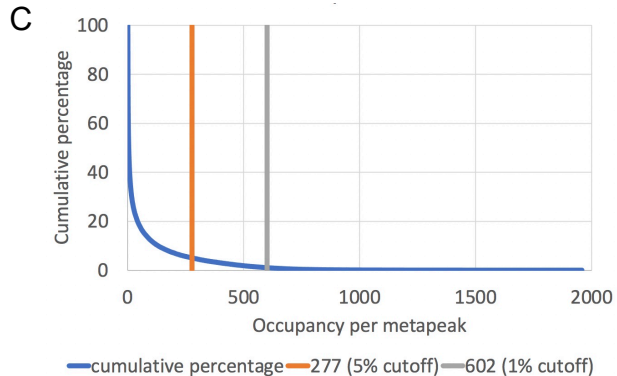


Metapeak occupancy

Worm

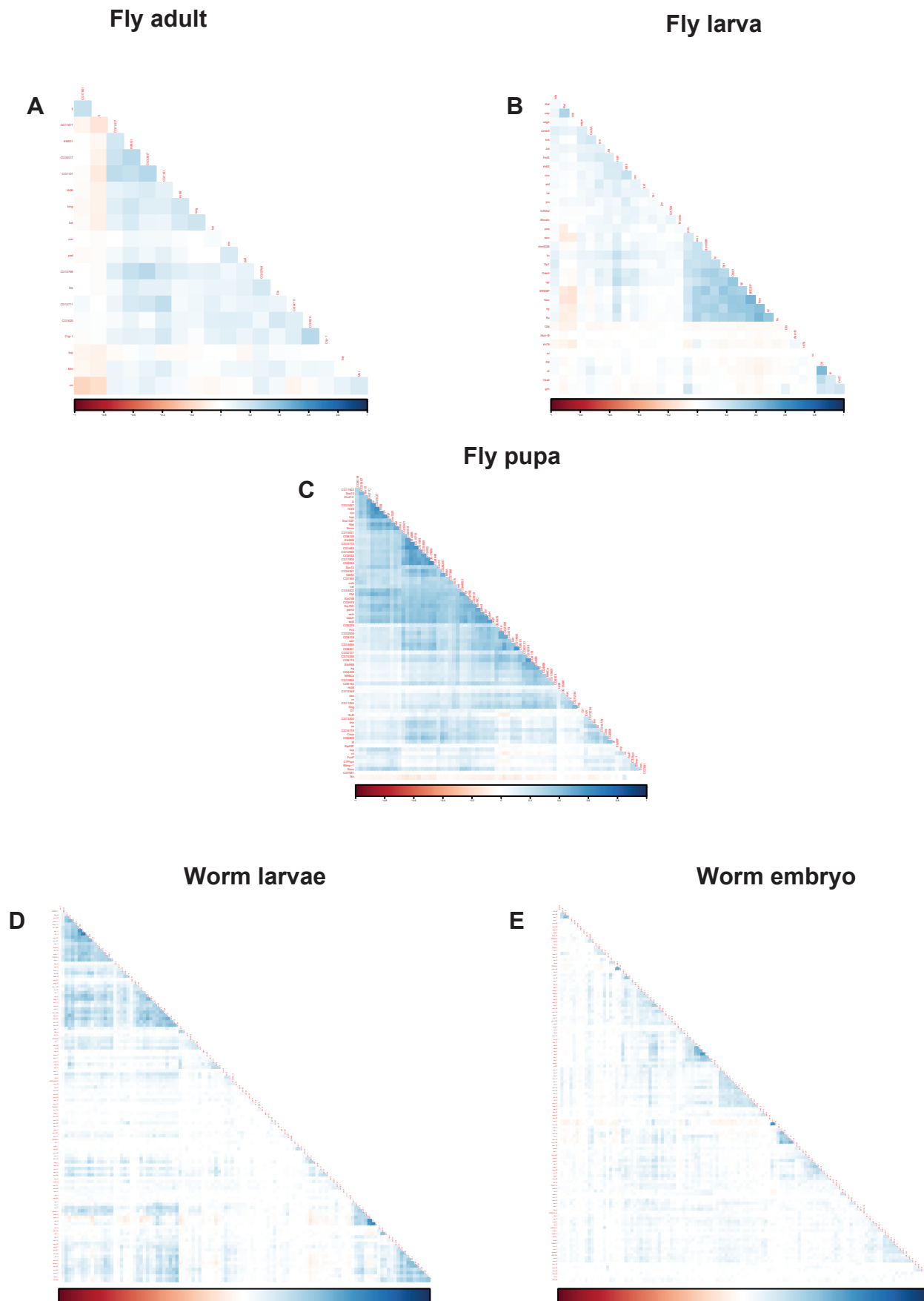


Fly



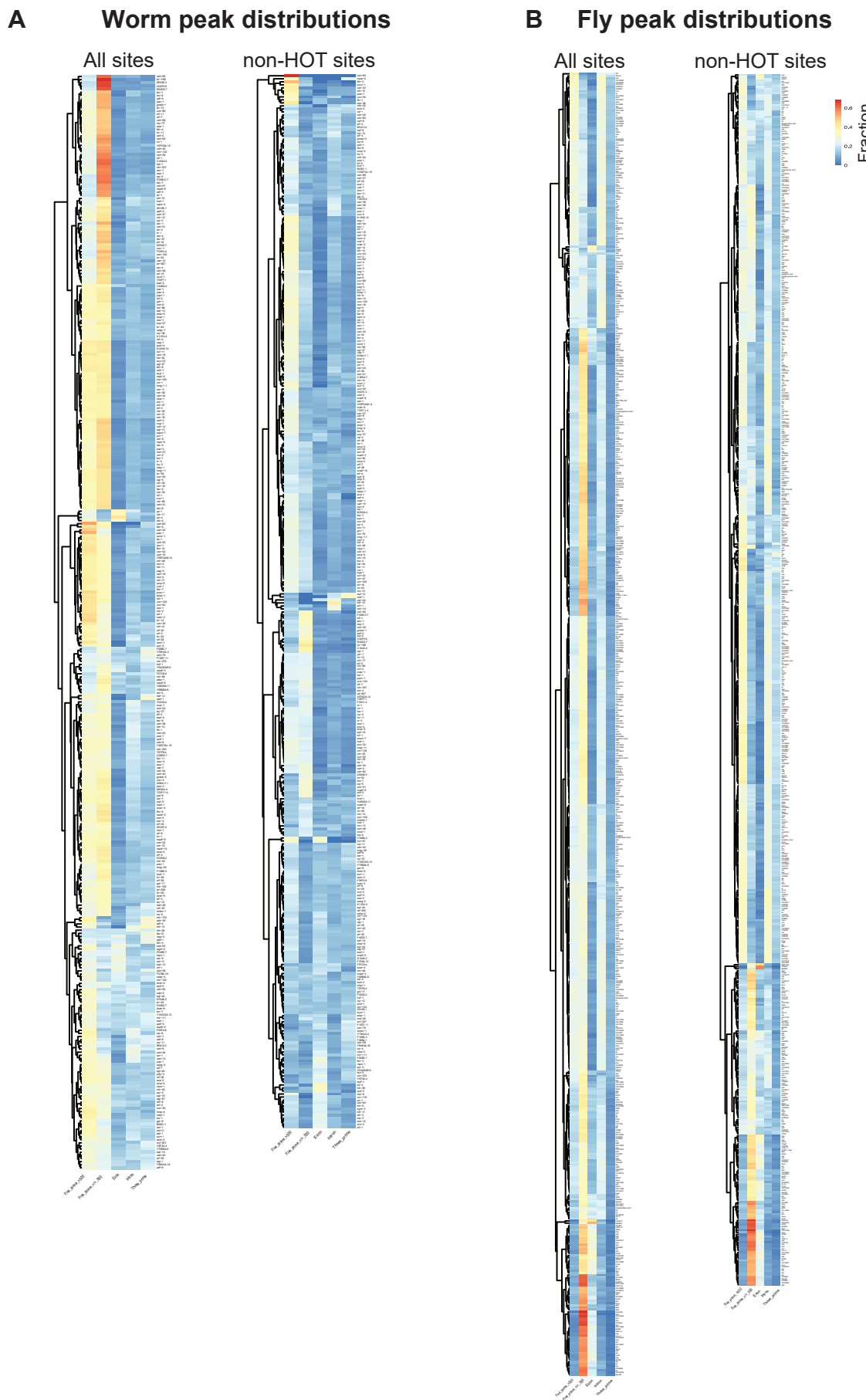
Supplemental Figure 3. HOT site thresholding. **A.** Comparison of HOT site thresholds based on using 1% and 5% of transcription factors assayed in our data to those identified using the Araya et al (2014) approach (labeled as “number of metapeaks $\geq\%$ simulated cutoffs”) and the kernel density estimation approach (L. Ma and A. Victorsen, unpublished; labeled as “number of metapeaks hotter than top % of simulations”). **B.** Decreasing cumulative percentage metapeaks as a function of occupancy per metapeak, with 5% (HOT) and 1% (UltraHOT) thresholds indicated by vertical lines (orange and gray respectively). **C.** As in **B**, but for fly metapeaks.

Supplemental Figure 4



Supplemental Figure 4. Correlation of TF-TF pairs. **A.** Pearson correlations of TFs in metapeaks in fly adult; **B** fly larva; **C** fly pupa; **D** worm larvae and **E** worm embryo. In addition to the clusters of correlated TFs (blue), note also the negative correlations (red).

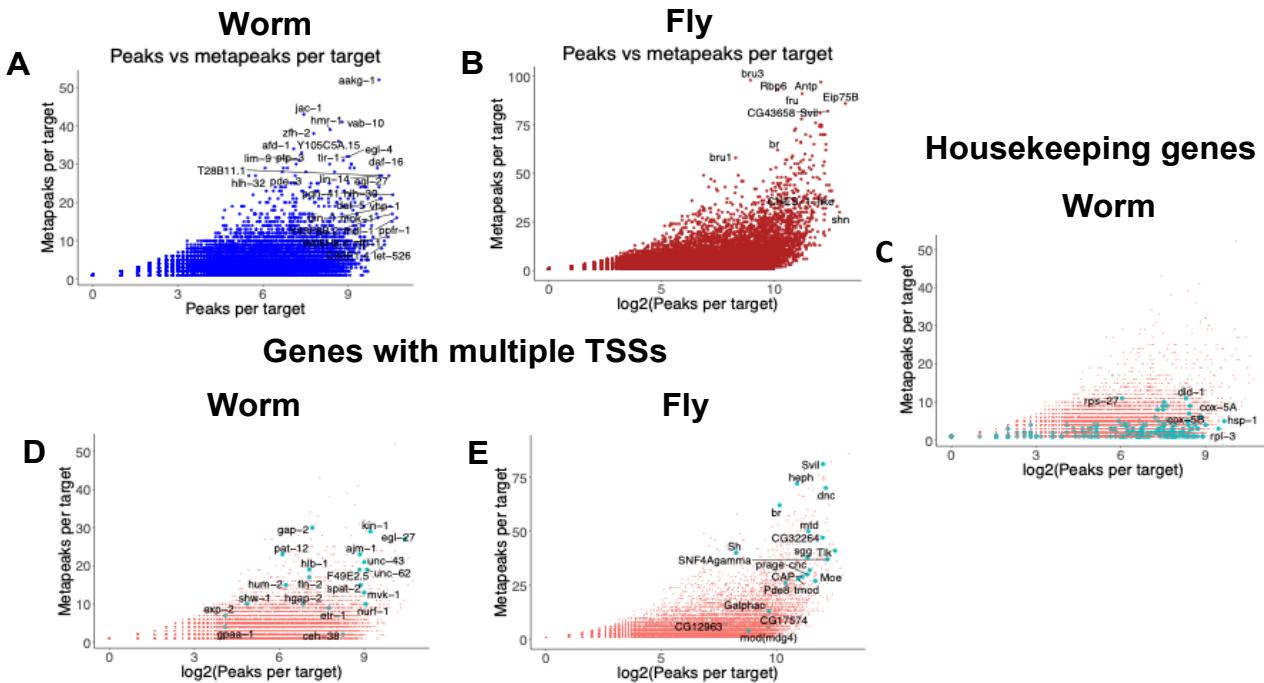
Supplemental Figure 5



Supplemental Figure 5. Peak distribution across gene features. **A.** Heat maps of the peak distribution of worm TFs with all peaks shown (left) and after HOT sites were removed (right). **B.** Heat maps of the peak distribution of fly TFs with all peaks shown (left) and after HOT sites were removed (right).

Supplemental Figure 6

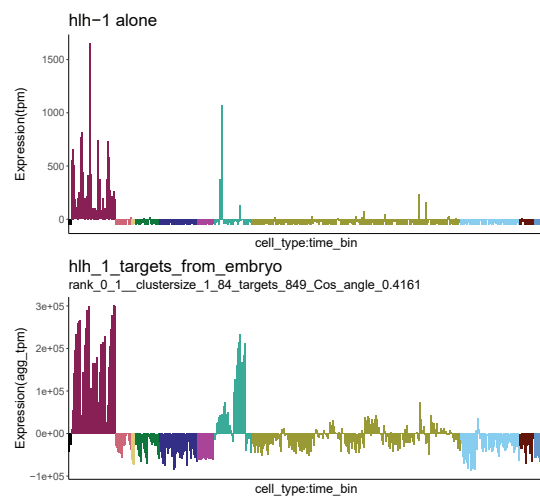
Peaks versus metapeaks per target



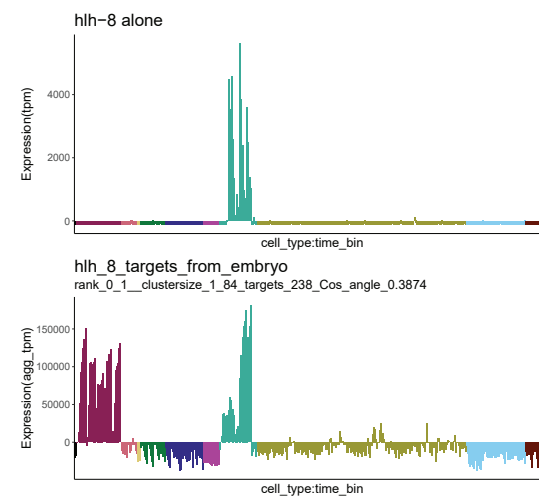
Supplemental Figure 6. Peak-metapeak properties. **A,B** Targets in worm (A) and fly (B) can have large numbers of peaks distributed in multiple metapeaks, suggesting complex regulation. Two genes (Myo81F and Pzl) with more than 100 assigned metapeaks were omitted. **C.** In worms a small set of carefully curated housekeeping genes often have only a few, often very large metapeaks. **D,E** In both worms (D) and flies (E) genes with multiple TSSs have multiple metapeaks, together containing high numbers of peaks.

Supplemental Figure 7

A



B

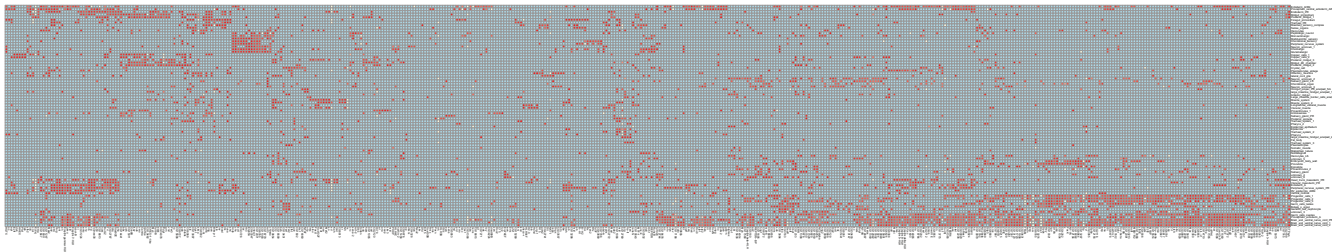


Supplemental Figure 7. TF-target gene relationships. Some targets can be shared between different TFs. **A.** The TF hh-1 is expressed in body wall muscles and the GLR mesodermal cells. The aggregate target expression is found there and also in other mesodermal cells. **B.** The TF hh-8 is specifically expressed in mesodermal cells and the aggregate target expression is found there and in body wall muscle cells. The similarity of the target profiles imply shared targets and indeed *ost-1* and *pat-10*, expressed in both sets of cell types, are targets of both TFs.

Supplemental Figure 8

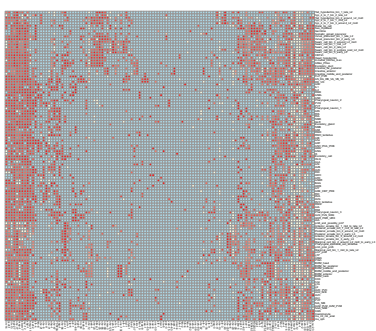
Fly embryo

A



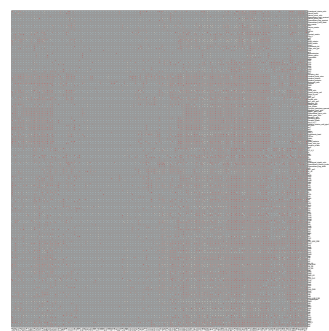
Worm larval stages

B



Worm L4/yAd

C



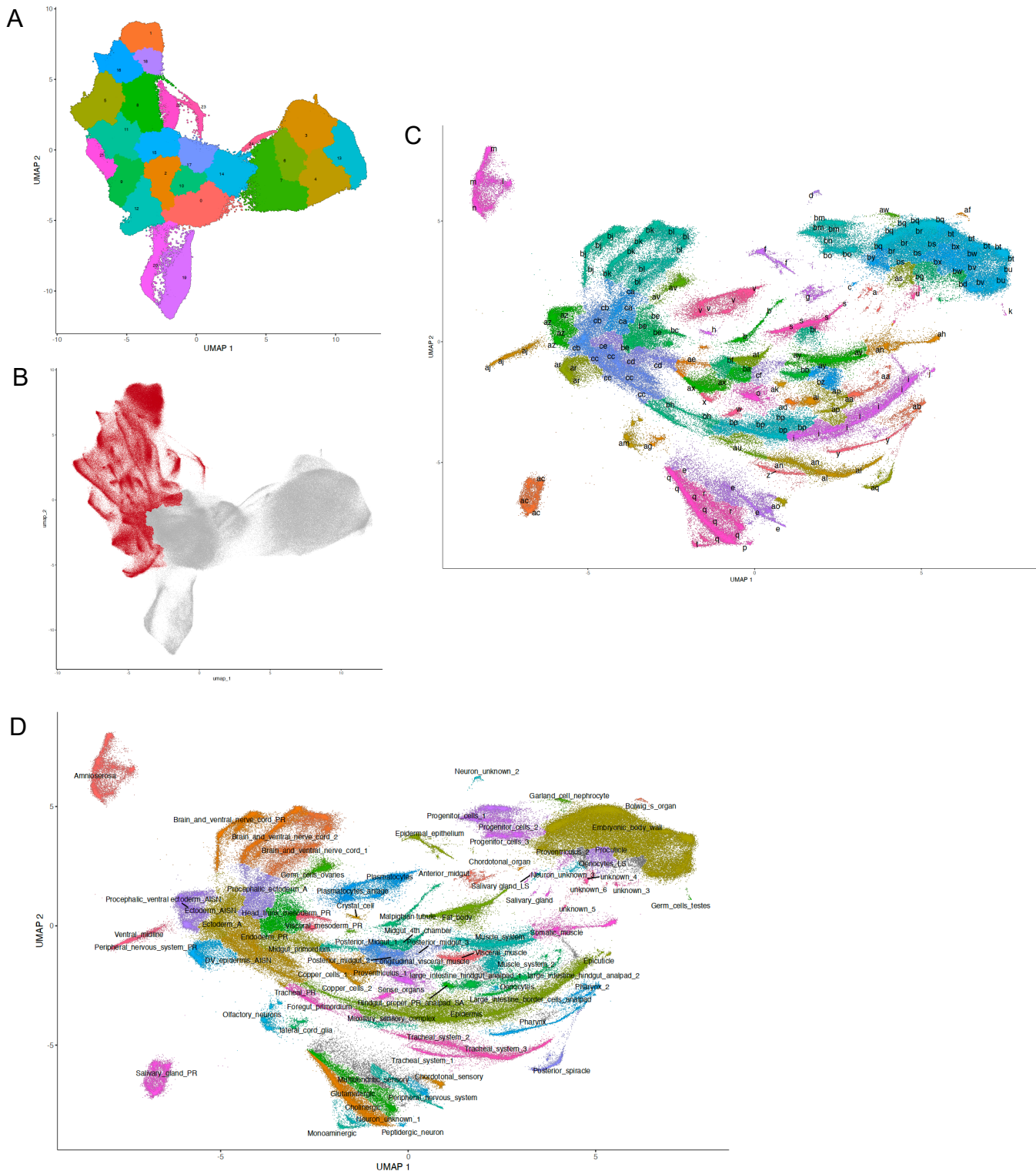
Worm embryo lineage

D



Supplemental Figure 8. The relative importance of TFs in cell type gene expression. **A.** Heatmap showing the importance of individual TFs for predicting target gene expression patterns in single cell types for: the fly embryo; **B.** the worm larval stages; **C.** the worm L4 and adult stages; and **D.** the lineage of the worm embryo. Color scale as in Figure 7. HTML version of these maps are available on the modERN website.

Supplemental Figure 9



Supplemental Figure 9. Reannotation of the fly single cell RNA-seq data set. **A.** UMAP of cells from Calderon et al., 2022. **B.** Older cells (red) were remapped to produce the relationships shown in **C**. **C.** Cells were clustered and then clusters were grouped as putative cell types and marker genes for each group were determined. **D.** The annotated cell types, determined by comparing the markers with the *in situ* database and literature.

Supplemental Table 1.

	Factor	Stage	IDR	Binding sites	Relative expression
OP563	CEBP-1	YA	0.69	4160	OP > RW
RW12290	CEBP-1	YA	1.27	1969	
OP436	MADF-5	L4	1.04	844	OP = RW
RW12308	MADF-5	L4	1.02	1145	
OP578	UNC-3	LE	1.1	639	OP < RW
RW12259	UNC-3	LE	1.01	631	
OP37	PHA-4	L4	1.03	1484	OP = RW
RW12220	PHA-4	L4	1.02	2947	
OP797	FLT-1	EE	1.11	1083	OP > RW
	FLT-1	EE	1.08	2849	

EE – early embryo; LE – late embryo
OP lines were generated by fosmid bombardment and RW strains were generated by CRISPR.

Supplemental Table 1. Comparison of five fosmid-based and CRISPR designed worm TF strains. ChIP-seq results and expression patterns of fosmid-based and CRISPR-generated TF worm strains.